MODIFIED SVPWM SWITCHING SCHEMES FOR HARMONIC SUPPRESSION IN FIVE PHASE VSI FED INDUCTION MOTOR DRIVE

D. Raja
Associate Professor,
Department of Electrical and Electronics Engineering,
Sri Manakula Vinayagar Engineering College,
Madagadipet, Puducherry -605107,India

G. Ravi
Professor,
Department of Electrical and Electronics Engineering
Pondicherry Engineering College
Pillaichavady, Puducherry – 605014, India

Abstract: *Power electronic converters play a major role in electric drives and their controls. Multi-phase motors are popular for various electric drive applications. This enables us to use the multi-phase AC machines than 3-ϕ machines. The multiphase AC drives are fed from voltage source inverters (VSIs) and it requires a suitable PWM method of control. This paper presents the various space vector PWM (SVPWM) techniques for 5-ϕ VSI fed 5-ϕ Induction Motor (IM) drives. Modified SVPWM switching techniques are introduced based on medium, large and the combined effect of medium and large vectors, which provides the operation with reduced % THD in the output voltages. Various switching schemes for 5-ϕ VSI fed 5-ϕ IM drive is investigated in terms of harmonics present in the output voltage. MATLAB Simulation results are included in this paper to show and verify the theoretical concepts.*

Keywords: *SVPWM; 5-ϕ Voltage Source Inverter; 5-ϕ Induction Motor; THD*

1. Introduction

In general, multi-phase systems have many advantages and they are used in applications such as automotive industry, aeronautic and electric power generation due to a variety of benefits provided by multi-phase drives over 3-ϕ drives. [1]. In case of even number phases, the poles are coinciding with each other and it will reduce the motor performance. So, odd number phases are preferred over even number phases [2]-[3]. Also, the output power of 5-ϕ system is greater than that of the 3-ϕ system. This has attracted the interest in the development of multi phase machines [4], [5].

The broad choice of switching techniques can be used for the VSI to produce the expected output [6]-[9]. The techniques start with sin triangle PWM, conventional SVPWM, and modified SVPWM. SVPWM technique is the more suitable for multiphase VSI and the no. of vectors increase with the no. of levels and no. of phases. [10], [11].

A 2 level VSI has 32 vectors represented into d_1-q_1 & d_3-q_3 subspaces. All subspaces are a source of lower order harmonics except the d_1-q_1 subspace. The switching techniques proposed in [12] can eliminate the harmonics present in d_3-q_3. In addition, this method can generate a sinusoidal phase voltage waveform. There are few SVPWM techniques proposed for the harmonic reduction [13] and for minimizing the switching losses of a 3-ϕ VSI and multilevel inverters [14]-[16]. Certain modifications are required in the switching scheme to reduce the harmonics in the output voltage of 5-ϕ VSI.

The SVPWM with modified switching scheme is proposed in this paper for the 5-ϕ VSI fed IM drive. The MATLAB/ Simulink is used to construct the system. The performances of proposed techniques are compared for 5-ϕ VSI fed IM drive.

2. Modeling of Five-Phase Induction Motor

Mathematical model can be represented for an induction motor. The 5-ϕ system variables are transformed into 2-ϕ variables in d-q plane rotating with synchronous speed. Displacement between two phases is 72 degrees and the number of phases must be the same before and after the transformation. The relationships between 5-ϕ and 2-ϕ variables are as follows.

$$V^s_{dq=} K_S\, V^s_{abcde}$$
$$i^s_{dq=} K_S\, i^s_{abcde}$$
$$\Psi^s_{dq=} K_S\, \Psi^s_{abcde} \quad (1)$$
$$V^r_{dq=} K_r\, V^r_{abcde}$$
$$i^r_{dq=} K_r\, i^r_{abcde}$$
$$\Psi^r_{dq=} K_r\, \Psi^r_{abcde} \quad (2)$$

Where,

$$K = \sqrt{\frac{2}{5}}\begin{bmatrix} 1 & \cos\left(\frac{2\pi}{5}\right) & \cos\left(\frac{4\pi}{5}\right) & \cos\left(\frac{4\pi}{5}\right) & \cos\left(\frac{2\pi}{5}\right) \\ 0 & \sin\left(\frac{2\pi}{5}\right) & \sin\left(\frac{4\pi}{5}\right) & \sin\left(\frac{4\pi}{5}\right) & \sin\left(\frac{2\pi}{5}\right) \\ 1 & \cos\left(\frac{4\pi}{5}\right) & \cos\left(\frac{8\pi}{5}\right) & \cos\left(\frac{8\pi}{5}\right) & \cos\left(\frac{4\pi}{5}\right) \\ 0 & \sin\left(\frac{4\pi}{5}\right) & \sin\left(\frac{8\pi}{5}\right) & -\sin\left(\frac{8\pi}{5}\right) & -\sin\left(\frac{4\pi}{5}\right) \\ \frac{1}{\sqrt{2}} & & \frac{1}{\sqrt{2}} & \frac{1}{\sqrt{2}} & \frac{1}{\sqrt{2}} & \frac{1}{\sqrt{2}} \end{bmatrix} \quad (3)$$

'K' is the 5-ϕ induction machine decoupling transformation matrix given in equation 2. The 5-ϕ machine is represented in d-q-x-y-o arbitrary plane. The d-q components are responsible for power generation, fluxes and torque production in the machine. System losses are accounted by x-y components and the reason for zero components being used is to show unchanged in the system. The 5-ϕ IM is modelled in the MATLAB simulink and the characteristics responses are obtained.

Essential machine model equations for stator sides and rotor sides in stationary reference frame are represented as follows:

$$V_{ds} = R_s i_{ds} + p\Psi_{ds}$$
$$V_{qs} = R_s i_{qs} + p\Psi_{qs} \quad (4)$$
$$\Psi_{xs} = L_{ls} i_{xs}$$
$$\Psi_{ys} = L_{ls} i_{ys} \quad (5)$$
$$V_{dr} = R_r i_{dr} + p\Psi_{dr}$$
$$V_{qr} = R_r i_{qr} + p\Psi_{qr} \quad (6)$$
$$\Psi_{xr} = L_{lr} i_{xr}$$
$$\Psi_{yr} = L_{lr} i_{yr} \quad (7)$$

Flux Linkage equations for stator and rotor sides are expressed as follows:

$$\Psi_{xs} = L_{ls} i_{xs} \qquad \Psi_{xr} = L_{lr} i_{xr} \quad (8)$$
$$\Psi_{ds} = (L_{ls} + L_m) i_{ds} + L_m i_{dr}$$
$$\Psi_{qs} = (L_{ls} + L_m) i_{qs} + L_m i_{qr} \quad (9)$$
$$\Psi_{dr} = (L_{lr} + L_m) i_{dr} + L_m i_{ds}$$
$$\Psi_{qr} = (L_{lr} + L_m) i_{qr} + L_m i_{qs} \quad (10)$$
$$\text{Where, } L_s = L_{ls} + L_m \qquad L_r = L_{lr} + L_m \quad (11)$$
$$\Psi_{ys} = L_{ls} i_{ys} \qquad \Psi_{yr} = L_{lr} i_{yr} \quad (12)$$

The equation for torque can be denoted as:

$$T_e = PL_m(i_{dr} i_{qs} - i_{ds} i_{dr}) \quad (13)$$
$$w_r = \int \frac{P}{2J}(T_e - T_L) \quad (14)$$

3. TWO-LEVEL FIVE-PHASE VSI

Multiphase IM drives are used for variable speed applications. The conventional multiphase VSI does not suitable for this application owing to the high amount of harmonics presented in the voltage waveforms. To reduce the harmonics, a space vector concept is used with modified switching sequence and also to maximize the fundamental voltage.

Fig.1 shows the circuit diagram for 5-ϕ VSI fed 5-ϕ IM drive comprises ten power switches, two switches per leg. The pole voltage is equal to V_{dc} when the upper switch is ON and it is zero when it is OFF. To avoid the direct short circuit of same leg switches, they switched opposite to each other.

Phase to neutral voltages (V_a ~ V_e) of 5-ϕ VSI can be expressed in terms of inverter pole voltages as given in equation (15) and (16) [12].

$$V_j = \frac{4}{5}V_j - \frac{1}{5}\sum_{i,i\neq j}^{5} V_j, \text{ if } j < 5 \quad (15)$$
$$V_j = \frac{4}{5}V_j - \frac{1}{5}\sum_{i,i\neq j}^{4} V_j, \text{ if } j = 5 \quad (16)$$

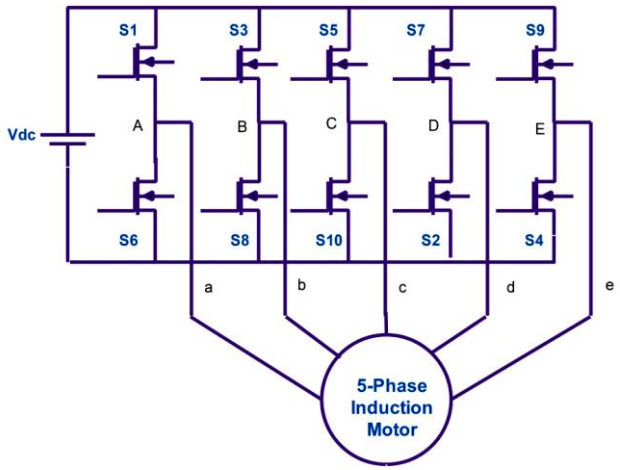

Fig. 1 5-ϕ VSI fed 5-ϕ IM drive

In general, a 5-ϕ 2-level VSI has 32 combinations of switching states (ie, 2^n, where n is the number of phases) and can be represented in two space vector planes (d_1-q_1 and d_3-q_3) includes thirty active and two zero vectors.

Binary numbers are used to represent the states on each space vectors. Bit '0' represents that the lower switch is ON while bit '1' represents that the upper switch is on. The three coordinated decagons formed by 30 active vectors originate at the 2 zero vectors. Inner, middle and outer decagons magnitudes are 0.2472, 0.4, and 0.6472.

Fig 2 and fig. 3 shows the space vector representation in d-q plane. The phase sequence in d_1q_1 is ABCDE while in d_3q_3 it is ACEBD. The middle decagon is the same in both subspaces while the inner and outer decagons are interchanged between d_1q_1 and d_3q_3. Equation (17) and (18) represents the 5-ϕ inverter voltage in two-phase d-q

plane. The value of a, a2, a3, & a4 is given in equation (19) to (22).

$$V_{d1q1} = \frac{2}{5}V_{dc}[V_a + aV_b + a^2V_c + a^3V_d + a^4V_e] \quad (17)$$

$$V_{d3q3} = \frac{2}{5}V_{dc}[V_a + aV_c + a^2V_e + a^3V_b + a^4V_d] \quad (18)$$

$$a = \cos\frac{2\pi}{5} + \sin\frac{2\pi}{5} \quad (19)$$

$$a^2 = \cos\frac{4\pi}{5} + \sin\frac{4\pi}{5} \quad (20)$$

$$a^3 = \cos\frac{4\pi}{5} - \sin\frac{4\pi}{5} \quad (21)$$

$$a^4 = \cos\frac{2\pi}{5} - \sin\frac{2\pi}{5} \quad (22)$$

4. SVPWM Switching Schemes for 5-ϕ VSI

A. Switching Scheme I: Using Medium Vectors in (d_1q_1 plane)

The medium decagon of d_1q_1 plane is considered in this elementary space vector (SV) modulation switching scheme for 5-ϕ VSI. The switching vector rotates in an anti-clockwise direction starting from V_{16} until V_{30} is reached as shown in Fig. 2. The equations (23), (24) & (25) used to calculate the conduction time in each switching state. Fig. 4 (a) & (b) shows the upper IGBT switching pattern in each phase and the respective switching vector has shown in Fig. 5 (a). In the first switching scheme (SS-1), the switching vectors start from 16, 29, 31, 31, 29 and 16 for one switching cycle T_s in sector I. while in the second switching scheme (SS-2), switching vector starts from 0, 16, 29, 31, 31, 29, 16 and 0. The magnitude used for one half of switching cycle is 0.5 times of t_o & t_{31} and 0.325 times of t_{am} and t_{bm}. as shown in fig. 4 (a) & (b). Fig. 5 (b) & (C) shows the modulating signals for both the switching schemes.

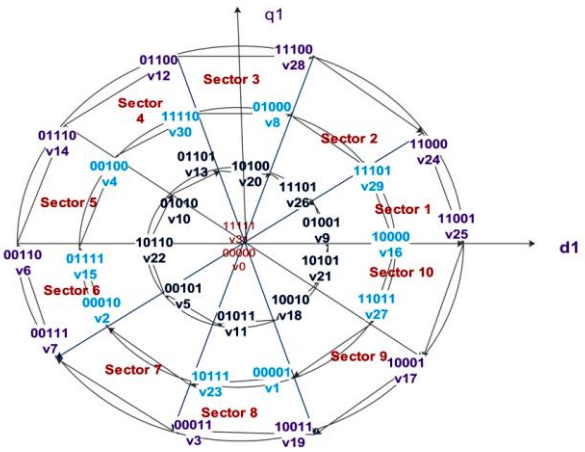

Fig. 2 Switching vectors in d_1-q_1 Subspace

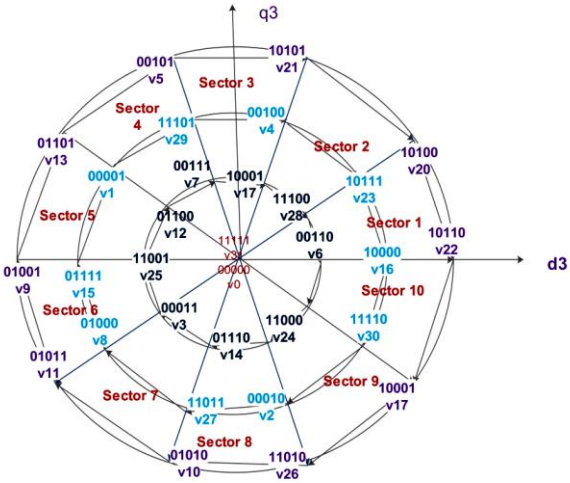

Fig. 3 Switching vectors in d_3-q_3 Subspace

The following expressions are used to calculate the conduction time t_{am}, t_{bm} and t_o.

$$t_{am} = \frac{|V_{ref}|\sin\left(\left(K\frac{\pi}{5}\right)-\theta\right)}{V_m\sin\left(\frac{\pi}{5}\right)}t_s \quad (23)$$

$$t_{bm} = \frac{|V_{ref}|\sin\left(\theta-\left((K-1)\frac{\pi}{5}\right)\right)}{V_m\sin\left(\frac{\pi}{5}\right)}t_s \quad (24)$$

$$t_0 = \frac{t_s - t_{am} - t_{bm}}{2} \quad (25)$$

Maximum possible fundamental peak voltage of large space vector is

$$V_{max} = |V_m|\cos\frac{\pi}{10}V_{dc} = 0.3804V_{dc} \quad (26)$$

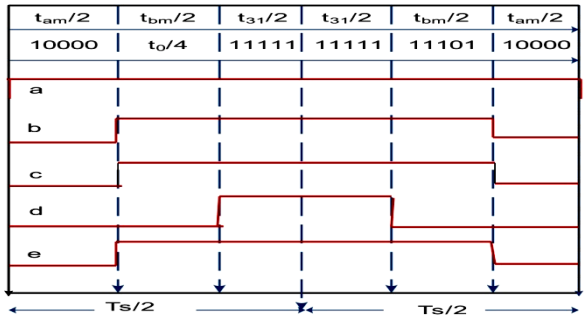

(a)

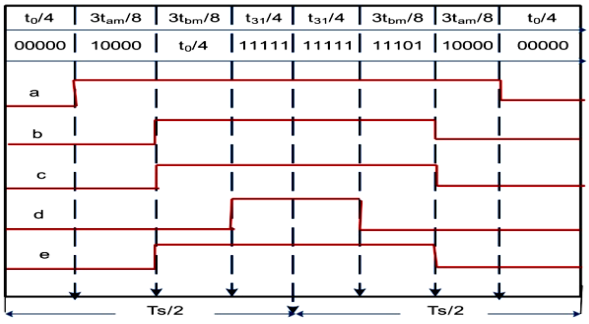

(b)

Fig. 4 switching pattern for Medium vectors in d_1-q_1 Subspace in Sector -I (a) SS -1 (b) SS-2

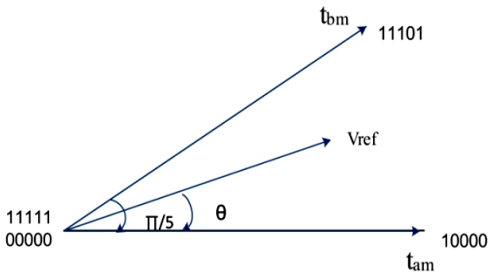

(a)

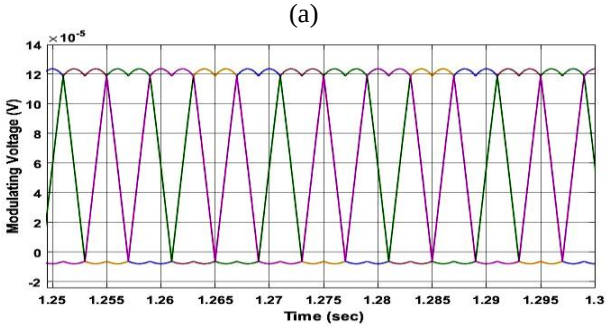

(b)

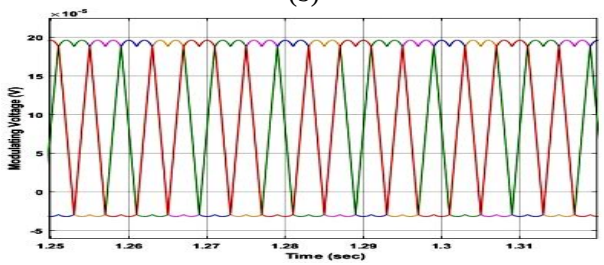

(c)

Fig.5 (a) Time Switching for Medium vectors in d_1-q_1 Subspace in Sector -I (b) & (c) Modulating signal for SS-1 & SS-2

B. Switching Scheme II:Using Large Vectors (d_1q_1 plane)

The Space Vectors in the large decagon of d_1q_1 plane are considered. The switching vector rotates in an anti-clockwise direction starting from V_{25} until V_{17} as shown in Fig. 2. The equations (27), (28) & (29) used to calculate the conduction time in each switching state. Fig. 6 (a) & (b) shows the upper IGBT switching pattern in each phase and the respective switching vector has shown in Fig. 7 (a). In the first switching scheme (SS-1), the switching vectors start from 25, 24, 31, 31, 24 and 25 for one switching cycle T_s in sector I. while in the second switching scheme (SS-2), switching vector starts from 0, 25, 24, 31, 31, 24, 25 and 0. The magnitude used for one half of switching cycle is 0.5 times of t_o & t_{31} and 0.325 times of t_{al} and t_{bl}. as shown in fig. 6 (a) & (b). Fig. 7 (b) & (C) shows the modulating signals for both the switching schemes.

The following expressions are used to calculate the conduction time t_{al}, t_{bl} and t_o.

$$t_{al} = \frac{|V_{ref}|\sin\left(\left(K\frac{\pi}{5}\right)-\theta\right)}{V_l \sin\left(\frac{\pi}{5}\right)} t_s \quad (27)$$

$$t_{bl} = \frac{|V_{ref}|\sin\left(\theta-\left((K-1)\frac{\pi}{5}\right)\right)}{V_l \sin\left(\frac{\pi}{5}\right)} t_s \quad (28)$$

$$t_0 = \frac{t_s - t_{al} - t_{bl}}{2} \quad (29)$$

Maximum possible fundamental peak voltage of large space vector is

$$V_{max} = |V_l|\cos\frac{\pi}{10} V_{dc} = 0.6155 V_{dc} \quad (30)$$

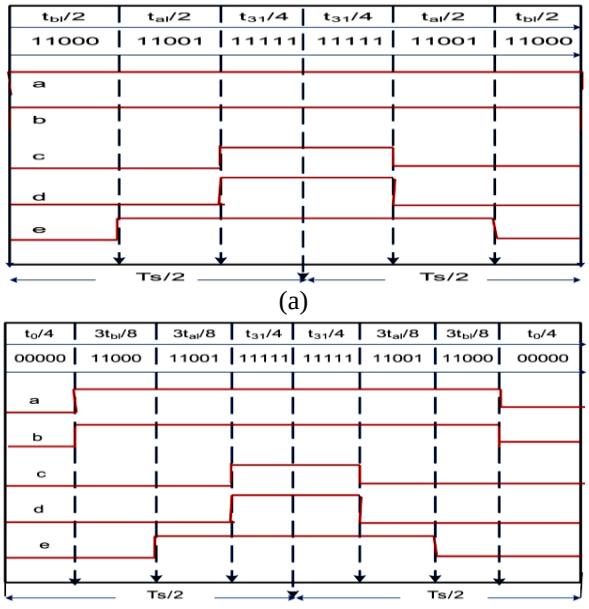

(a)

(b)

Fig. 6 switching pattern for large vectors in d_1-q_1 Subspace in Sector -I (a) SS-1 (b) SS-2

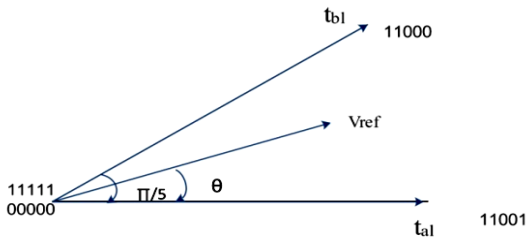

(a)

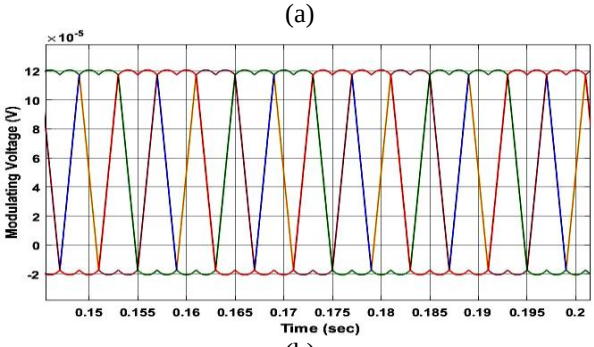

(b)

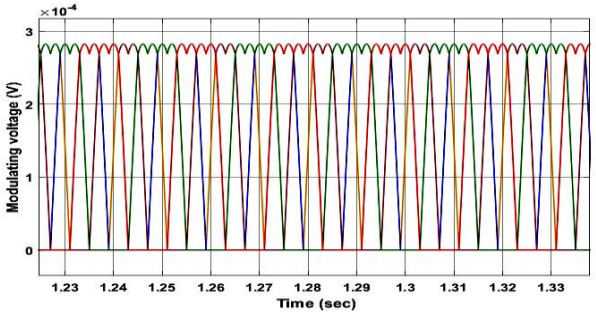

(c)

Fig.7 (a) Time Switching for Large vectors in d_1-q_1 subspace in Sector –I (b) & (c) Modulating signal for SS-1 & SS-2

C. Switching Scheme III: Using combination of medium and Large Vectors (d_1q_1 plane)

Instead of using only two active and two zero vectors, four active and two zero vectors can be used for the five phase VSI. Fig. 8 (a) & (b) shows the upper IGBT switching pattern in each phase and the respective switching vector has shown in Fig. 9 (a). In the first switching scheme (SS-1), the switching vectors start from 16, 24, 25,29,31,31,29,25,24 and 16 for one switching cycle T_s in sector I. while in the second switching scheme (SS-2), switching vector starts from 0, 16, 24, 25,29,31,31,29,25,24 16 and 0. The magnitude used for one half of switching cycle is 0.5 times of t_o & t_{31} and 0.325 times of t_{am}, t_{bm}, t_{al} and t_{bl} as shown in fig. 8 (a) & (b). Fig. 9 (b) & (C) shows the modulating signals for both the switching schemes.

The following expressions are used to calculate the conduction time t_{am}, t_{bm}, t_{al}, t_{bl} and t_o.

$$t_a = t_{al} + t_{am} \quad (31)$$

$$t_b = t_{bl} + t_{bm} \quad (32)$$

The Maximum possible fundamental peak voltage of combinations of medium and large space vector is

$$|V_m|\cos\frac{\pi}{10}V_{dc} \le V_{max} \le |V_l|\cos\frac{\pi}{10}V_{dc} \quad (33)$$

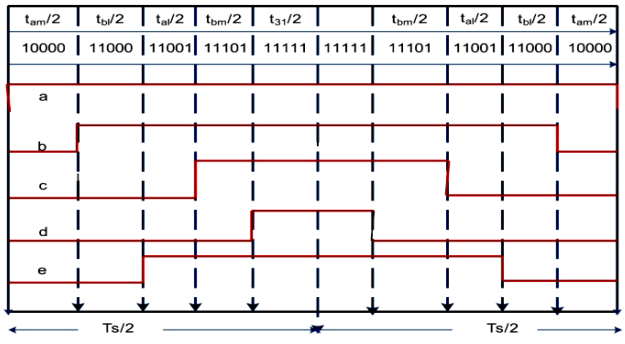

(a)

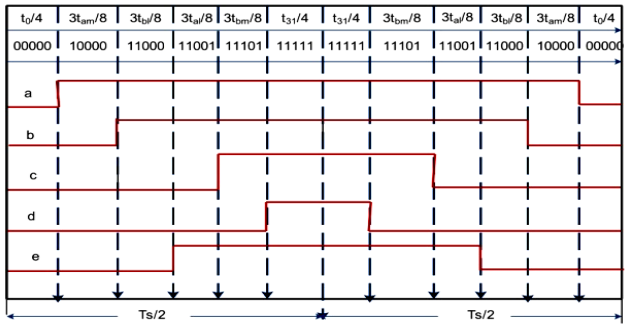

(b)

Fig. 8 switching pattern for combination of medium and Large Vectors in d_1-q_1 Subspace in Sector -I (a) SS-1 (b) SS-2

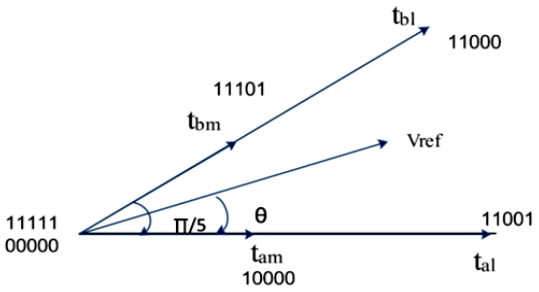

(a)

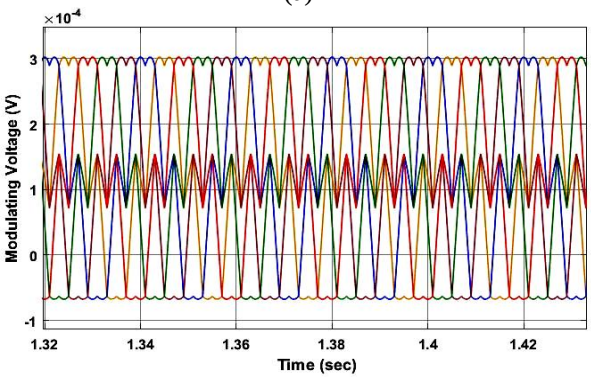

(b)

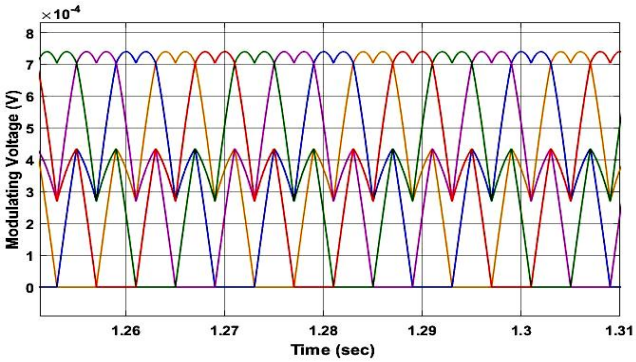

(c)

Fig.9 (a) Time Switching for combination of medium and Large Vectors in d_1-q_1 Subspace in Sector –I (b) & (c) Modulating signal for SS-1 & SS-2

D. Switching Scheme IV: Using Large Vectors (d_3q_3 plane)

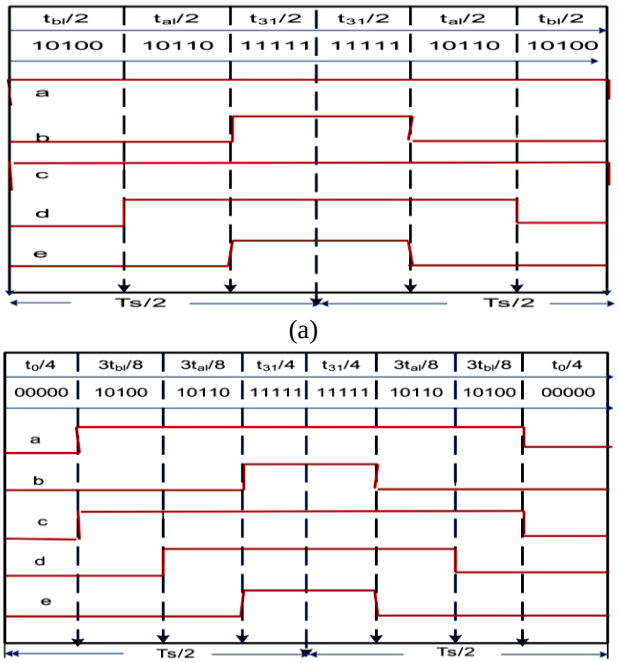

(a)

(b)

Fig. 10 switching pattern for large vectors in d_3-q_3 Subspace in Sector -I (a) SS-1 (b) SS-2

The SVs in large decagon of d_3q_3 plane are considered. The switching vector rotates to the in an anti-clockwise direction starting from V_{22} until V_{17} as shown in Fig. 3. The equation (27), (28) & (29) are used to calculate the conduction time in each switching state. Fig. 10 (a) & (b) shows the upper IGBT switching pattern in each phase and the respective switching vector has shown Fig. 11 (a). In the first switching scheme (SS-1), the switching vectors start from 20, 22, 31, 31, 22 and 20 for one switching cycle T_s in sector I. while in the second switching scheme (SS-2), switching vector starts from 0, 20, 22, 31, 31, 22, 20 and 0. The magnitude used for one half of switching cycle is 0.5 times of t_o & t_{31} and 0.325 times of t_{al} and t_{bl}. as shown in fig.10 (a) & (b). Fig. 11 (b) & (C) shows the modulating signals for both the switching schemes.

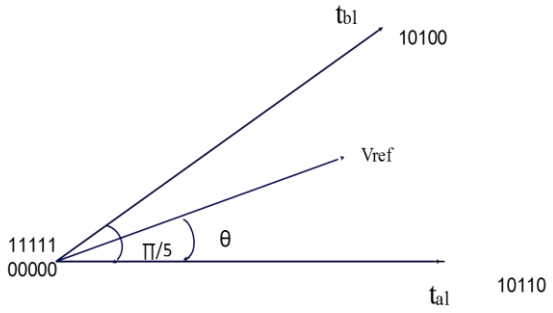

(a)

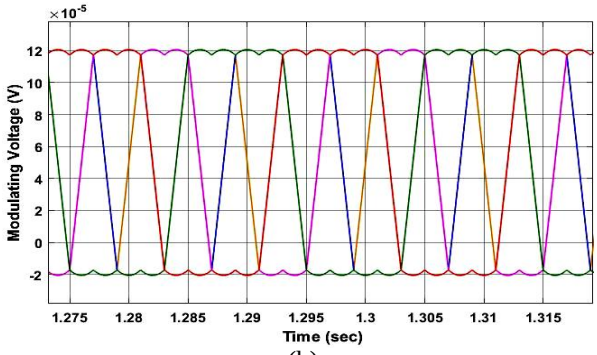

(b)

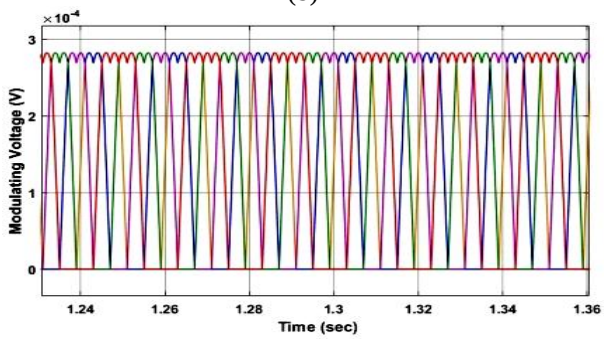

(c)

Fig.11 (a) Time Switching for Large vectors in d_3-q_3 Subspace in Sector –I (b) & (c) Modulating signal for SS-1 & SS-2

E. Switching Scheme V: Using combination of medium and Large Vectors (d_3q_3 plane)

The fundamental subspaces ABCDE are mapped into the order of vectors while ACEBD is the order in auxiliary subspace. In a certain sector of the fundamental subspace of fig.2, the outer decagon vector aligns with middle decagon and falls diagonally opposite to each other in an auxiliary subspace of fig. 3. If the state duration of medium vector and a large vector is same, harmonics will be eliminated due to the zero resulting vectors in auxiliary subspace.

Fig. 12 (a) & (b) shows the upper IGBT switching pattern in each phase and the respective switching vector has shown in Fig. 13 (a). In the first switching scheme (SS-1), the switching vectors start from 16, 20, 22,23,31,31,23,22,20 and 16 for one switching cycle T_s in sector I. while in the second switching scheme (SS-2), switching vector starts from 0, 16, 20, 22,23,31,31,23,22,20,16 and 0. The magnitude used for one half of switching cycle is 0.5 times of t_o & t_{31} and 0.325 times of t_{am}, t_{bm}, t_{al} and t_{bl} as shown in fig. 12 (a) & (b). Fig. 13 (b) & (C) shows the modulating signals for both the switching schemes.

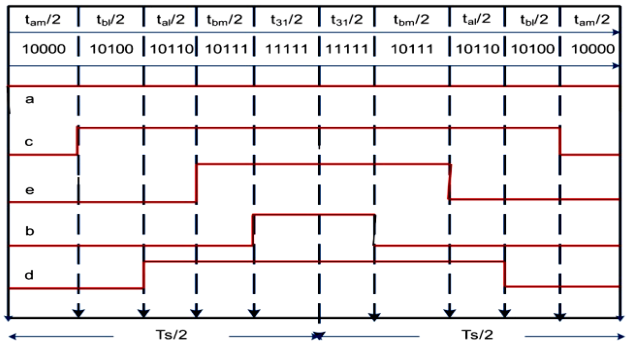

(a)

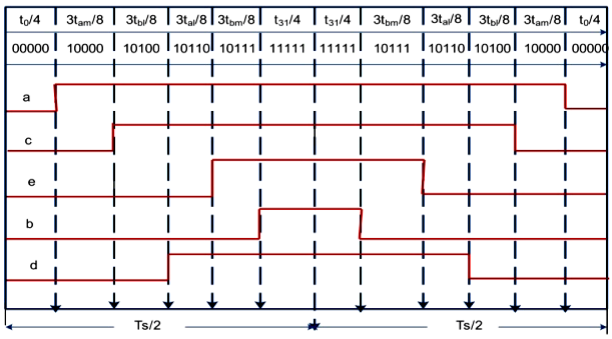

(b)

Fig. 12 switching pattern for combination of medium and Large Vectors in d_3-q_3 Subspace in Sector -I (a) SS-1 (b) SS-2

5. SIMULATION RESULTS

A MATLAB Simulink software simulation used to determine the effect of SV based switching techniques and to compare the results of various switching techniques such as medium vector, large vector and the grouping of a medium and large vector in d_1-q_1 and d_3-q_3 subspace. Table 1 lists the simulation parameters of the system and the performance characteristics are as shown in fig. 14. The load torque variations are as shown in fig. 14 (c) at 0.5 sec, 1 sec and 1.5 sec of 2 Nm, 3 Nm, and 4 Nm and the respective rotor current variations are as stated in fig.14 (d).

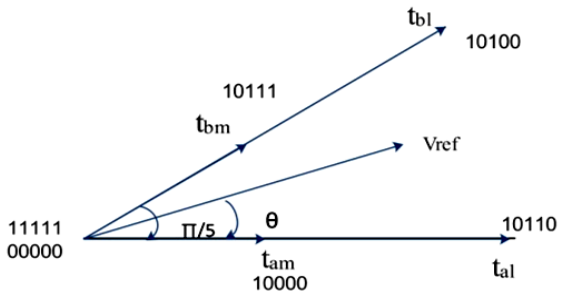

(a)

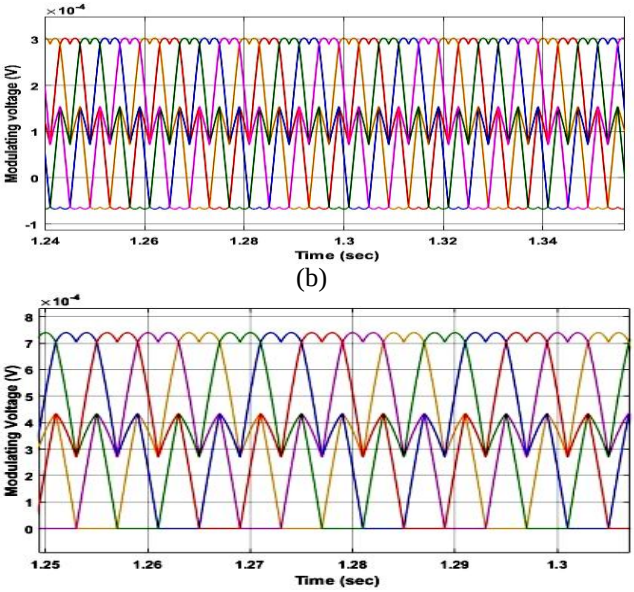

Fig. 13 (a) Time Switching for combination of medium and Large Vectors in d_3-q_3 Subspace in Sector –I (b) & (c) Modulating signal for SS-1 & SS-2

Table 1
Parameters of 5-ϕ VSI fed IM Drive

Parameters	Values
DC Bus voltage	400 V
Switching frequency	5 KHz
Modulation index	1
Power (P)	1 hp
Motor RMS Input Voltage (V)	220
No. of Phases	5
Number of Poles (p)	4
Resistance (stator)	10.1 Ω
Inductance (stator)	0.833 Henry
Resistance (rotor)	9.854 Ω
Inductance (rotor)	0.782 Henry
Mutual Inductance	0.782 Henry
Inertia	0.0088

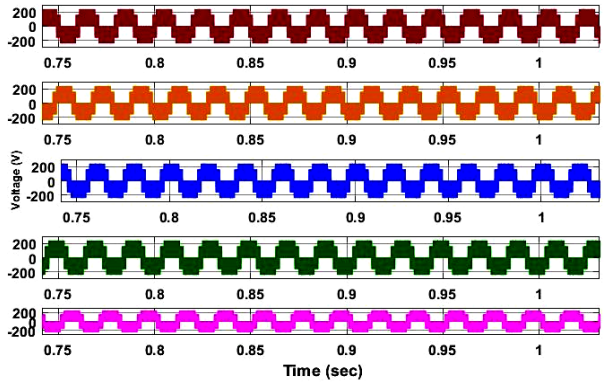

(a)

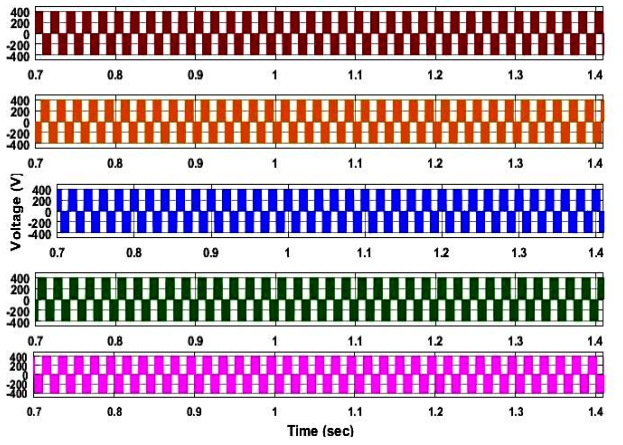

(b)

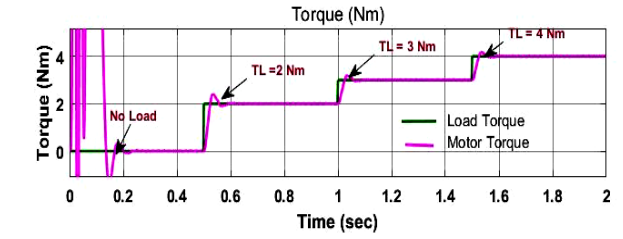

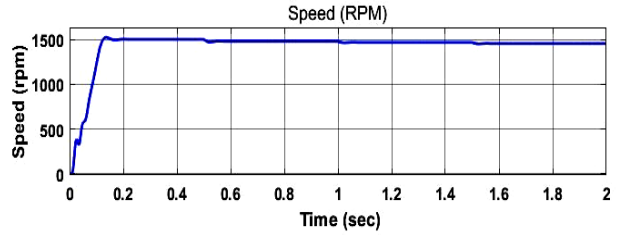

(c)

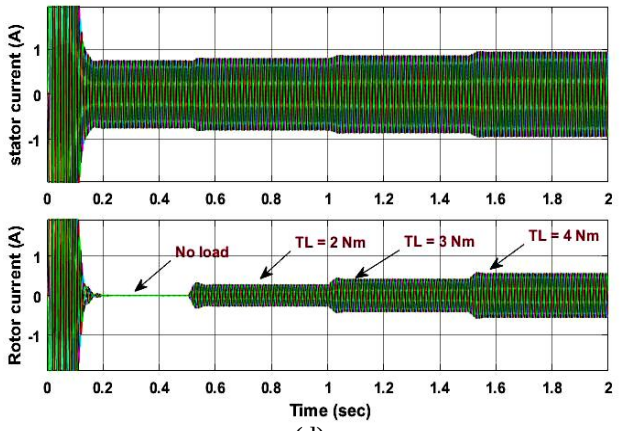

(d)

Fig. 14 Performance characteristics of 5-ϕ SVPWM VSI fed IM Drive (a) Phase Voltage (b) Line Voltage (c) Speed & torque response (d) stator & rotor current

The % THD in a phase and line voltage of 5-ϕ SVPWM VSI fed IM drive for different switching schemes shown in fig. 15 (a) to (d). From these figures, d_3-q_3 large vector switching scheme (SS-2) produces the lowest THD in line and phase voltages when compared to other switching vectors. Lower order harmonic such as 3rd order and 7th order harmonics variations for different switching schemes are as reported in fig. 16 (a) to (d). From these figures, lower order harmonics minimization in large vector switching is a maximum when compared to the other three types of switching vectors.

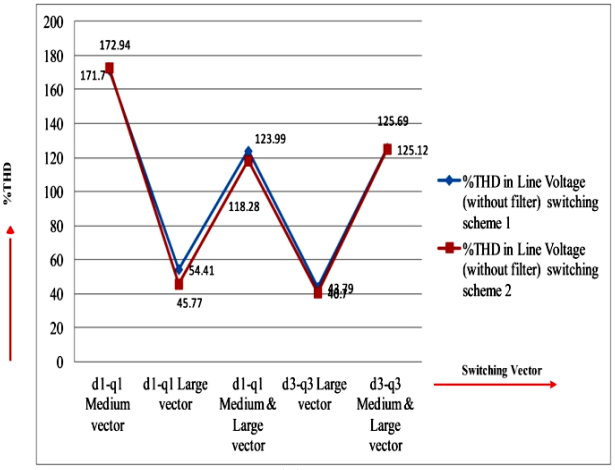

(a)

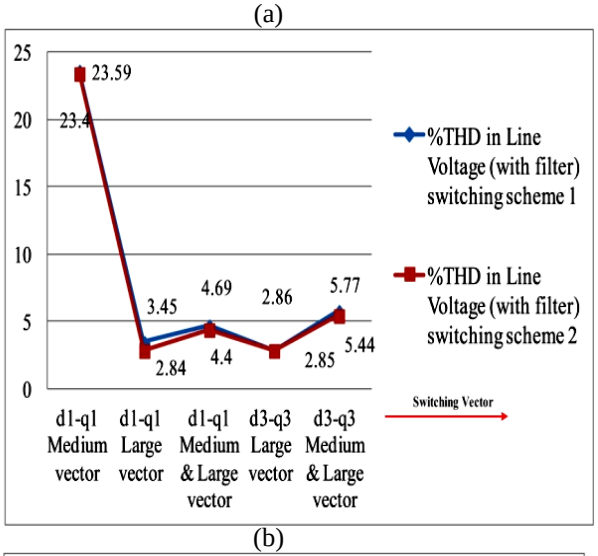

(b)

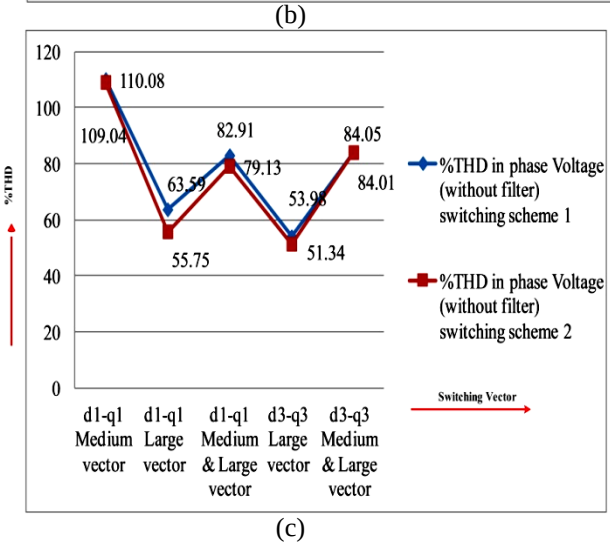

(c)

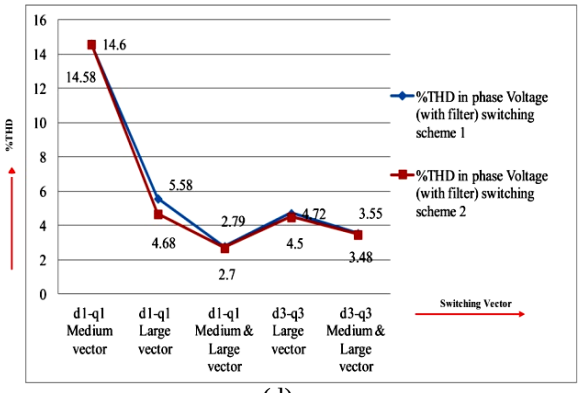

(d)

Fig. 15 (a) % THD in Line voltage without filter (b) % THD in Line voltage with filter (c) % THD in phase voltage without filter (d) % THD in phase voltage with filter for different SVPWM switching scheme

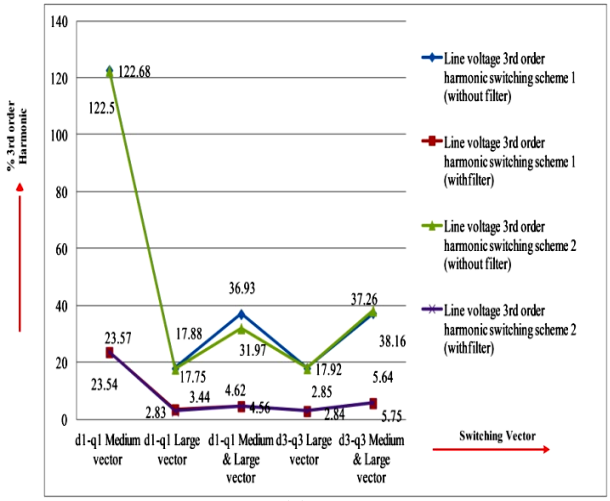

(a)

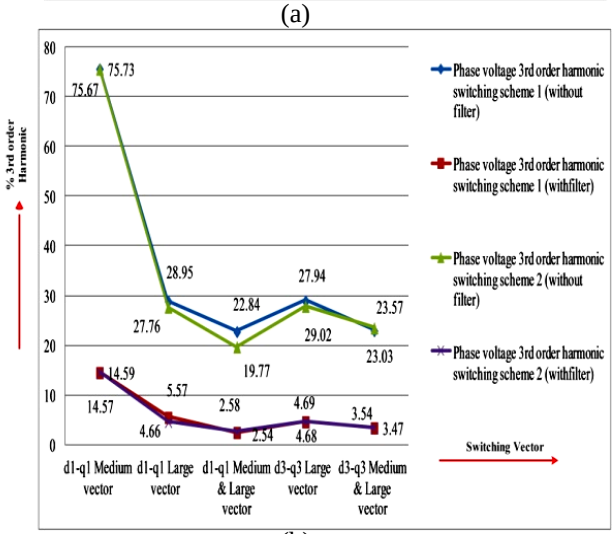

(b)

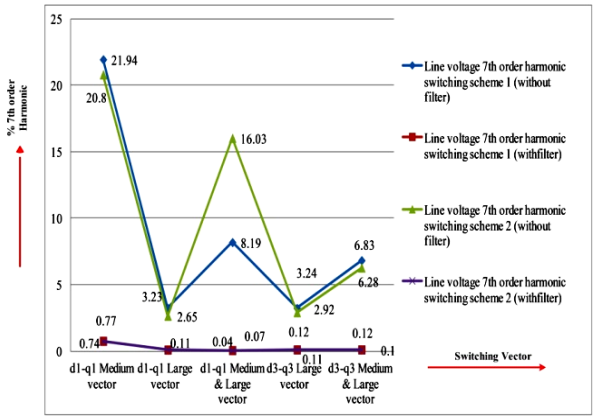

(c)

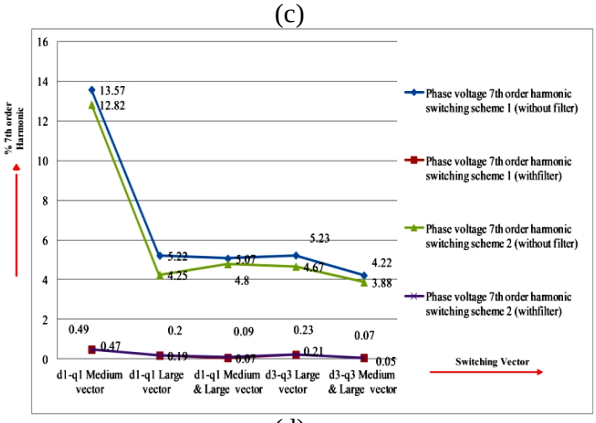

(d)

Fig. 16 (a) 3rd order harmonics in Line voltage (b) 3rd order harmonics in phase voltage (c) 7th order harmonics in Line voltage (d) 7th order harmonics in phase voltage for different SVPWM switching scheme

6. CONCLUSION

This paper focused on improving the input voltage quality of 5-ϕ induction motor by proposing a 5-ϕ VSI with various modified SVPWM techniques. Use of SVPWM techniques improves the utilization of DC bus voltage when compared to Sinusoidal PWM techniques. Two different switching schemes are designed for five different space vector combinations in d_1q_1 and d_3q_3 subspaces. This investigation is performed in the MATLAB Simulink for 5-ϕ VSI fed IM drive. The overall comparison result shows that switching scheme (SS-2) for d_1q_1 and d_3-q_3 large vector gives the superior performance in terms of reduction in harmonics of phase and line voltages than other methods. From the fig. 15 and 16, the harmonic minimization in a line and phase voltage using d_3q_3 large vector switching scheme (SS-2) is superior when compared to d_1q_1 large vector switching schemes.

References:

1. Subodh Kanta Barika, Kiran Kumar Jaladi *"Five-Phase IM DTC-SVM sche. with PI Control. & ANN control."* Publi. by Elsevier Ltd in Procedia Tech. 25 (2016) 816 – 823.
2. K. B. Yadav, Alok Kumar Mohanty, Prabhat Kumar, *"Recent Research Trend on Multi-phase Induction Machines"* Proc. of Int. Conf. on Control, Communi. and Power Engg., CCPE, Elsevier- 2014. pp. 580 -586.
3. K.S. kumar, Das. A, Ramchand. R, Patel.C & K. G.kumar, *"A 5-level inv. scheme for a 4-pole IM drive by feeding the identical voltage-profile windgs from both sides,"* IEEE Tra. Indu. Electr., vol. 57, no. 8, pp. 2776–2784, Aug. 2010.
4. A. S. A Khalik, S. Ahmed, A. A. E, & A. Massoud, *"Effect of stator wdg connection of 5-ϕ IM on Torque Ripples Under Open Line Condition"*, IEEE Tran.. Mechatronic, vol. 20, no. 2, pp. 580–593, April. 2015.
5. C. Heising, M. Oettmeier, R. Bertlet, J. Fang, V. Staudt & A. Steimel, *"Simu. of a symm. Fault of a 5-ϕ IM used in Naval appl."*, IEEE con., pp. 1298-1303, Sep. 2009.
6. E.Levi *" Multi ϕ IM drive – a technolo. tatus review"* IET Elec.. Pow. App. Vol. 1, No.4, pp.489-516, July 2007.
7. B. Jyothi, Venu.M, G. Rao & T. Karthik, *" Modeling & Simulation of 5-ϕ IM Fed with 5-ϕ Inverter Topolo."* IJS&T, Vol 8(19), August 2015.
8. MK K Sahu, AK K Panda, BP Panigrahi *"DTC for 3-Level NPC Inverter-Fed IM Drive"* ETASR – Engg., Tech. & Applied Science Res. Vol. 2, No. 2, 2012, 201-208.
9. B. Jyothi and Dr.M.Venu Gopala Rao "*Comparison of Five Leg Inv. and Five Phase Full Bridge Inv. for Five Ph. Supply"*, Int. Conf. on ISEG 19-20 Sept. 2014.
10. A. Iqbal, S. Moinuddin and M. R. Khan, *"Space Vector Model of A Five-Phase Voltage Source Inverter,"* 2006 IEEE International Conference on Industrial Technology, Mumbai, 2006, pp. 488-493.
11. S. Moinoddin and A. Iqbal, *"Space vector model of a five-phase current source inverter,"* 2016 Biennial International Conference on Power and Energy Systems: Towards Sustainable Energy (PESTSE), Bangalore, 2016, pp. 1-6.
12. Wan Noraishah, Wan Abdul Munim, Mohd Firdaus Ismail, Ahmad Farid Abidin, and Harizan Che Mat Haris, *"Multi-phase Inverter Space Vector Modulation",* IEEE 7th International power engg. Optimization conf., 3-4 june 2013, pp.149-154.
13. Mahmoud Gaballah, Mohammed El-Bardini, *"Low cost digital signal generation for driving space vector PWM inverter"*, Ain Shams Engineering Journal, Volume 4, Issue 4, 2013, Pages 763-774, ISSN 2090-4479.
14. Nanda Kumar, S., Vijayan, S. & Nanda Kumar, E.*" Asymmetric SVM Technique for Minimizing Switching Loss of Inverter"* Arabian Journal for Science and Engineering (2014) 39: 3123.
15. Devisree Sasi , Jisha Kuruvilla P , Anish Gopinath, *"Generalized SVPWM Algorithm for Two Legged Three Phase Multilevel Inverter"*, International Journal of Power Electronics and Drive System (IJPEDS) Vol.3, No.3, September 2013, pp. 279-286 ISSN: 2088-8694.
16. D. Zhao, V.S.S.P.K. Hari, G. Narayanan and R. Ayyanar, *"Space-Vector-Based Hybrid Pulse width Modulation Tech. for Reduced Harmonic Distortion and Switching Loss,"* in *IEEE Trans. on Power Electr*, vol. 25, no. 3, pp. 760-774, March 2010.